ment being toward higher values of the potential. The potential was computed as proportional to the local density of cells. The latter case was treated as a random walk of cells. We have designed a new parameter in order to check whether cell migration is due to the presence of an attraction/repulsion potential resulting from the local cell density.

Our results militate against a global (density-based) attraction model based on the idea of a universal attraction of cells by each other. We must, therefore, conclude that such a model does not constitute a valid explanation for the formation of clusters observed experimentally with noninvasive cell lines. The alternative, i.e., a random migration of cells until two cells with agglomerative properties meet each other to form the embryo of an aggregate, must be considered instead. These agglomerative properties, which are, thus, not shared by all of the cells of a population, remain to be evidenced experimentally.

References

[1] B. Nawrocki-Raby, M. Polette, C. Gilles, C. Clavel, K. Strumane, M. Matos, J.-M. Zahm, F. Van Roy, N. Bonnet, and P. Birembaut, "Quantitative cell dispersion analysis: New test to measure tumor cell aggressiveness," *Int. J. Cancer*, vol. 93, pp. 644–652, 2001.

[2] M. Matos, B. Nawrocki-Raby, J.-M. Zahm, M. Polette, P. Birembaut, and N. Bonnet, "Cell migration and proliferation are not determinant factors in the *in vitro* sociologic behavior of bronchial epithelial cell lines," *Cell Motility Cytoskeleton*, vol. 53, pp. 53–65, 2002.

[3] G. B. Ermentrout and L. Edelstein-Keshet, "Cellular automata approaches to biological modeling," *J. Theor. Biol.*, vol. 160, pp. 97–133, 1993.

[4] E. Parzen, "Estimation of a probability density function and mode," *Ann. Math. Statist.*, vol. 33, pp. 1065–1076, 1962.

Effect of Skull Resistivity on the Spatial Resolutions of EEG and MEG

Jaakko A. Malmivuo* and Veikko E. Suihko

***Abstract*—The resistivity values of the different tissues of the head affect the lead fields of electroencephalography (EEG). When the head is modeled with a concentric spherical model, the different resistivity values have no effect on the lead fields of the magnetoencephalography (MEG). Recent publications indicate that the resistivity of the skull is much lower than what was estimated by Rush and Driscoll. At the moment, this information on skull resistivity is, however, slightly controversial. We have compared the spatial resolution of EEG and MEG for cortical sources by calculating the half-sensitivity volumes (HSVs) of EEG and MEG as a function of electrode and magnetometer distance, respectively, with the relative skull resistivity as a parameter. Because the spatial resolution is related to the HSV, these data give an overview of the effect of these parameters on the spatial resolution of both techniques. Our calculations show that, with the new information on the resistivity of the skull, in the spherical model for cortical sources the spatial resolution of the EEG is better than that of the MEG.**

***Index Terms*—Bioelectromagnetism, electroencephalography (EEG), magnetoencephalography (MEG).**

I. Introduction

THE electric activity of the brain generates both electric and magnetic fields, detected by electroencephalogram (EEG) and magnetoencephalogram (MEG). Both of these techniques are nowadays used as research and clinical tools. For the benefit of brain research, it is important to discuss the relative merits of these techniques. In this discussion, there exist several theoretical and technical issues. One of these issues is the spatial resolution.

We have previously demonstrated with calculations with the Rush–Driscoll model [8] that, if the relative resistivity of the skull is 80 times that of scalp and brain tissues, the half-sensitivity volume (HSV) of an MEG measured with the axial gradiometer is an order of magnitude larger than that of a bipolar EEG measurement. The HSV of a planar gradiometer MEG in the Rush–Driscoll model is of approximately the same order as that of the bipolar EEG. [3]–[6]. (To be accurate, at electrode and magnetometer distances shorter than 20 mm, the EEG had a smaller HSV.)

Several studies on the comparison of the spatial resolution of the EEG and the MEG have been published. Liu *et al.* have recently made an excellent review of this work [2]. In this paper, they also published their own study on this subject. They studied the spatial resolution of an EEG and MEG for a distributed source model with the Monte Carlo method. Though they used in their realistic head model the resistivity ratio of 80/1 for the skull, they found that the localization of the EEG is more accurate than that of the MEG.

It has recently been demonstrated with several different approaches that the earlier conception of the high resistivity of the skull is overestimated. In one study, it was found that the ratio between the resistivity

Manuscript received December 20, 2002; revised September 30, 2003. This work was supported by the Ragnar Granit Foundation. *Asterisk indicates corresponding author.*

*J. A. Malmivuo is with the Ragnar Granit Institute, Tampere University of Technology, FIN-33101 Tampere, Finland (e-mail: jaakko.malmivuo@tut.fi).

V. E. Suihko was with Ragnar Granit Institute Tampere University of Technology, FIN-33101 Tampere, Finland. He is now with the Departments of Clinical Neurophysiology and Diagnostic Radiology, Seinäjoki Central Hospital, FIN-60101 Seinäjoki, Finland (e-mail: veikko.suihko@epshp.fi).

Digital Object Identifier 10.1109/TBME.2004.827255

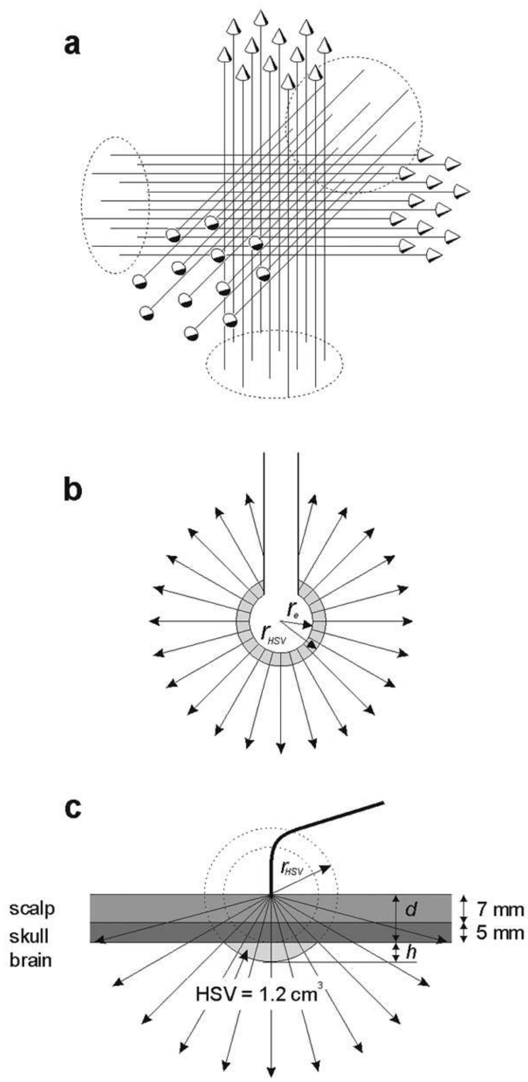

Fig. 1. Examples of the lead fields and HSVs for different lead configurations. (a) Dipolar lead has homogeneous sensitivity and the HSV equals the whole source region. (b) For a deep electrode, the $\mathrm{HSV} = 12 \cdot r_e^3$. (c) If a point electrode is on the surface of the scalp and the head is homogeneous, $\mathrm{HSV} = 0.688 \cdot d^3$. With the scalp and skull thickness of 1.2 cm, the HSV is approximately 1.2 cm^3.

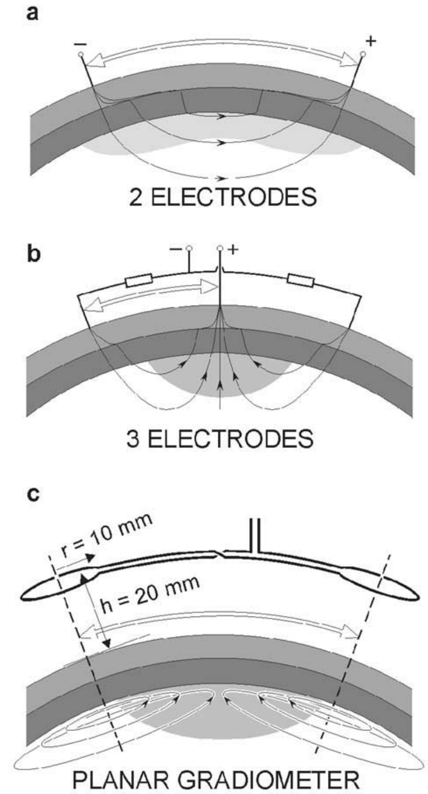

Fig. 2. Measurement configurations and dimensions for electric and magnetic leads: (a) two-electrode electric lead, (b) three-electrode electric lead, and (c) planar gradiometer magnetic lead. The HSVs are illustrated with light gray color. Note the tangential nature of the sensitivities of the two-electrode electric lead and planar gradiometer magnetic lead. The sensitivity of the three-electrode electric lead has a radial nature.

of the skull and that of the brain and scalp tissues is 15/1 [7]. Another study suggested that the ratio is only 8/1 [1].

We recalculated the most central results of our previous study with the relative skull resistivity ratio as a parameter to give for the reader more reliable information on the effect of the skull resistivity on the HSVs of the EEG and MEG.

II. HSV Concept

A. HSV as the Source Model

To investigate the EEG and MEG detectors' ability to concentrate their measurement sensitivity, we use the concept of half-sensitivity volume. Let us discuss the sensitivity of a single surface electrode. In the brain region, its sensitivity is highest just under it. Let us assume that the brain is a homogeneously distributed source, i.e., throughout the brain the neuronal sources have the same probability to activate in an instant of time and in direction. In such a situation, most of the signal comes from the region where the sensitivity is the highest, i.e., from just under the electrode. The faster the sensitivity decreases as a function of the distance from the electrode, the smaller the region is from where the signal comes, i.e., the better the spatial resolution is. To find a relationship between the fall off of the sensitivity as a function of distance and the spatial resolution we define the concept of HSV. The HSV is the volume of the source region in which the magnitude of the detector's sensitivity is more than one half of its maximum value in the source region [5]. The smaller the HSV is, the smaller the region is from which the detector's signal originates. The HSV concept concerns primarily the spatial resolution on the surface of the brain. In this paper, we do not discuss the detection of deep sources.

To clarify the concept of HSV, we give some examples.

B. Dipolar Leads

A dipolar lead, like the x, y and z leads of vector cardiography, has homogeneous sensitivity in the direction of the coordinate axis throughout the source region [see Fig. 1(a)]. The HSV of a dipolar lead is the whole source region and recording such dipolar leads gives no information on the source location.

C. Deep Electrodes

When recording the electric activity of the brain with an electrode in the brain region, the measurement sensitivity decreases proportional to the square of the distance from the electrode center [Fig. 1(b)]. If the spherical electrode tip radius is r_e, its surface is $4\pi r_e^2$. The distance

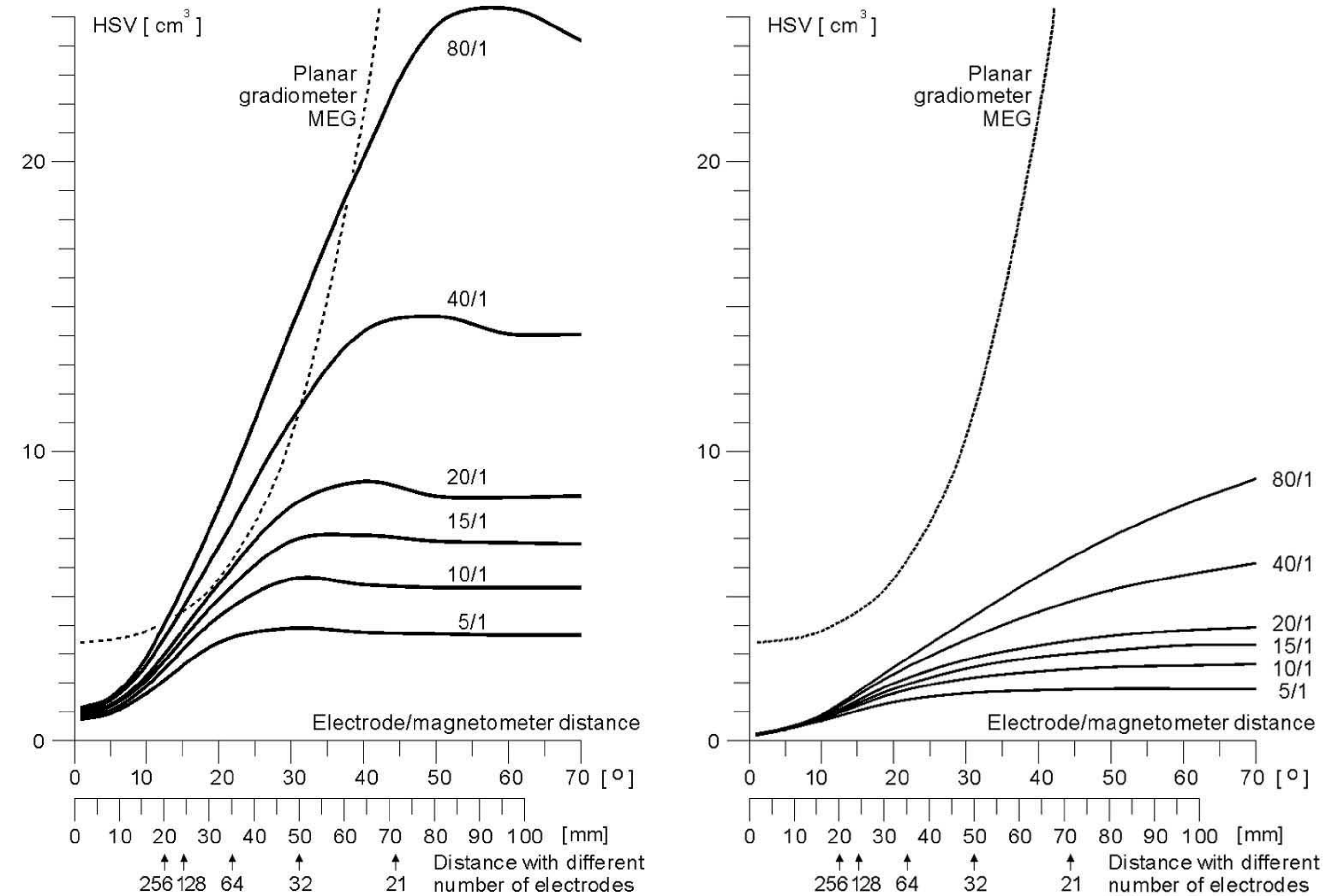

Fig. 3. HSVs of (a) two- and (b) three-electrode EEG and planar gradiometer MEG as a function of electrode and magnetometer distance, respectively. The relative skull resistivity is 5/1, 10/1, 15/1, 20/1, 40/1, and 80/1 for the skull/brain and scalp. The electrode distances for EEG lead systems with different numbers of leads are also indicated.

$r_{\rm HSV}$ where the spherical surface is double and the sensitivity is one half of that on the electrode surface is

$$4\pi r_{\rm HSV}^2 = 2\cdot 4\pi r_e^2 \quad \text{and } r_{\rm HSV} = \sqrt{2}\cdot r_e. \tag{1}$$

The HSV is then

$$\frac{4}{3}\pi r_{\rm HSV}^3 = \frac{4}{3}\pi(\sqrt{2}\cdot r_e)^3 = 11.84 r_e^3 \approx 12 r_e^3. \tag{2}$$

(To be accurate, the electrode volume in that region must be subtracted.)

If the electrode tip radius is 1 μm or 1 mm, the HSV is of the order of 12 μm^3 or 12 mm^3, respectively. If the electrode is located on the surface of the cortex, the HSV is, of course, half of that.

D. Homogeneous Head Model

Assume that the scalp, skull, and brain have the same resistivity. We approximate the head with a half space model [see Fig. 1(c)]. Assume that a point electrode is on the surface of the scalp. The maximum sensitivity of this electrode in the brain region is on the cortex just under the electrode. On the surface of a sphere with radius $\sqrt{2}\cdot d$, where d is the thickness of the scalp and skull, the sensitivity is one half of the maximum sensitivity. The HSV is the sphere segment whose volume is

$$\text{HSV} = \frac{1}{3}\cdot\pi h^2(3r_{\rm HSV} - h) \tag{3}$$

where

$$r_{\rm HSV} = \text{radius of the HSV sphere segment}$$
$$h = \text{height of the sphere segment.}$$

Inserting into (3) for the HSV radius $r_{\rm HSV} = \sqrt{2}\cdot d$ and noting that $h = r_{\rm HSV} - d$, we obtain

$$\text{HSV} = \frac{1}{3}\cdot\pi(4\sqrt{2}-5)d^3 = 0.688 d^3. \tag{4}$$

In the Rush–Driscoll model, the distance from the skin to the cortex $d = 1.2$ cm. Then the $\text{HSV} = 0.688\cdot 1.2^3$ cm^3 $=1.2$ cm^3.

E. Inhomogeneous Head Model

Let us model the head with an inhomogeneous spherical model. Assume that the skull has the resistivity of 5, 10, 15, 20, 40, or 80 times that of the scalp and brain. For one electrode, the calculated values of HSV are 1.8, 2.7, 3.5, 4.2, 7.0, and 12 cm^3, respectively. They may also be estimated from the HSV curves for the electrode configuration of Fig. 2(a) shown in Fig. 3(a). When the electrode distance increases up to 180°, the HSV curves approximately hold their value which they have at 70° in Fig. 3(a) [5, Fig. 8(a)]. Because this HSV value is for two electrodes, the value for one electrode is obtained by dividing that by two.

III. Methods

A. Head Model

For the head, we used the geometry of the Rush–Driscoll model with concentric spheres of 80-, 85-, and 92-mm radii for the outer surfaces of the brain, skull, and scalp, respectively [8]. Like Rush and Driscoll, we assumed that the brain and the scalp have the same resistivity. For the

TABLE I
HSV OF TWO- AND THREE-ELECTRODE EEG LEADS WITH DIFFERENT RELATIVE SKULL RESISTIVITY VALUES AND OF PLANAR GRADIOMETER MEG LEADS WITH $\mathrm{H} = 20$ MM AND $\mathrm{R} = 10$ MM. HSVS ARE GIVEN IN [CM^3] WITH DIFFERENT RELATIVE SKULL RESISTIVITIES

Electrode or Magneto-meter Distance		HSV for Two-electrode EEG [cm^3] HSV for Three-electrode EEG [cm^3]						HSV for Planar Gradiometer MEG
		Relative Skull Resistivity						
degree	mm	5/1	10/1	15/1	20/1	40/1	80/1	[cm^3]
1	1.6	0.74	0.83	0.92	1.00	1.09	1.14	3.40
		0.21	0.21	0.22	0.22	0.23	0.24	
5	8.0	0.96	1.07	1.20	1.23	1.41	1.51	3.50
		0.37	0.28	0.40	0.41	0.42	0.43	
10	16	1.66	1.92	2.10	2.25	2.62	2.91	3.80
		0.69	0.76	0.79	0.81	0.86	0.90	
20	32	3.38	4.28	4.90	5.42	6.72	8.07	5.60
		1.36	1.64	1.80	1.99	2.31	2.56	
30	48	3.90	5.61	6.90	8.11	11.06	14.26	10.51
		1.63	2.16	2.50	2.81	3.49	4.16	
40	64	3.66	5.40	7.10	8.96	14.16	20.15	21.67
		1.73	2.42	2.90	3.29	4.46	5.68	
50	80	3.68	5.33	6.80	8.46	14.67	24.68	40.75
		1.80	2.55	3.10	3.63	5.21	7.03	
60	96	3.66	5.28	6.90	8.42	14.06	25.31	64.42
		1.82	2.62	3.30	3.82	5.72	8.15	
70	112	3.64	5.32	6.80	8.47	14.05	24.21	
		1.82	2.65	3.30	3.94	6.14	9.07	

skull resistivity, the relative value of 80/1 given by Rush and Driscoll has recently been seriously questioned [1], [7]. Therefore, we used in our calculations the resistivity values of 5, 10, 15, 20, 40, and 80 times that of the brain and scalp. This gives the reader the possibility to evaluate the HSVs of the EEG and MEG with that resistivity value he/she considers to be correct.

B. EEG and MEG Leads Used

For the EEG, the HSV was calculated for bipolar and three-electrode leads with point electrodes as a function of the electrode distance [Fig. 3(a) and (b)]. These have tangential and radial sensitivities (see Fig. 2(a) and (b), respectively). For the MEG, the HSV was similarly calculated for a planar gradiometer as a function of the magnetometer distance [Fig. 3(a) and (b)]. The planar gradiometer has tangential sensitivity. The radii of the MEG coils were 10 mm and their distance from the scalp was 20 mm [Fig. 2(c)].

IV. RESULTS

The HSVs for two- and three-electrode EEGs and planar gradiometer MEG with skull/brain and scalp resistivity ratios of 5/1, 10/1, 15/1, 20/1, 40/1, and 80/1 as a function of electrode and magnetometer distance are given in Table I and Fig. 3(a) and (b). It will be observed that, with the realistic resistivity values for the skull, 5/1, 10/1, and 15/1, the HSV of the EEG is smaller than that of the MEG with all values of electrode and magnetometer distances.

The interesting area of the electrode distance is some 20 mm, corresponding to a 256-electrode high-resolution EEG system. In this region, the HSV of the bipolar EEG is about 50% smaller than that of the planar gradiometer MEG.

V. CONCLUSION

Our calculations show that, when adopting for the skull more realistic relative resistivity values of 5/1, 10/1, and 15/1, the HSV of the EEG is smaller than that of the MEG. This means that the EEG has better spatial resolution than the MEG.

VI. DISCUSSION

In comparing the EEG and MEG detectors' merits, the criterion has usually been either their accuracy in localizing a source dipole or in differentiating between two nearby dipoles. In a clinical measurement, however, a neurologist is interested in measuring the electric activity of brain tissue from a limited region. That is a volume source, not a discrete dipole. These are, of course, mathematically related concepts.

The high resistivity of the skull is the main factor affecting the spatial resolution of the EEG. The fact that this has no effect on the spatial resolution of the MEG has been the main reason for the belief that the MEG would provide better spatial resolution than the EEG.

We have previously shown that even with a relative value of 1/80 skull resistivity the HSV of the EEG is about the same size as that of the MEG. This means that the latter is not superior with respect to spatial resolution. Now the new information regarding the HSV of the EEG, based on more realistic resistivity values for the skull, indicates that the EEG apparently has better spatial resolution than the MEG.

REFERENCES

[1] R. Hoekema, G. J. M. Huiskamp, G. H. Wieneke, F. S. S. Leijten, C. W. M. van Veelen, P. C. van Rijen, and A. C. van Huffelen, "Measurement of the conductivity of the skull, temporarily removed during epilepsy surgery," *Biomedizinische Technik*, pp. 103–105, 2001. Band 46 B Ergänz. b. 2.

[2] A. K. Liu, A. M. Dale, and J. W. Belliveau, "Monte Carlo simulation studies of EEG and MEG localization accuracy," *Human Brain Mapping*, no. 16, pp. 47–62, 2002.

[3] J. Malmivuo and R. Plonsey. (1995) *Bioelectromagnetism—Principles and Applications of Bioelectric and Biomagnetic Fields*

[4] J. Malmivuo and J. Puikkonen, "Sensitivity distribution of multichannel MEG detectors," in *Proc. 6th Int. Conf. Biomagnetism*, Tokyo, Japan, Aug. 27–30, 1987, pp. 112–113.

[5] J. Malmivuo, V. Suihko, and H. Eskola, "Sensitivity distributions of EEG and MEG measurements," *IEEE Trans. Biomed. Eng.*, vol. 44, pp. 196–208, Mar. 1997.

[6] ——, "Correction to the sensitivity distributions of EEG and MEG measurements," *IEEE Trans. Biomed. Eng.*, vol. 44, p. 430, May 1997.

[7] T. F. Oostendorp, J. Delbecke, and D. F. Stegman, "The conductivity of the human skull: Results in vivo and in vitro measurements," *IEEE Trans. Biomed. Eng.*, vol. 47, pp. 1487–1492, Nov. 2000.

[8] S. Rush and D. A. Driscoll, "EEG-electrode sensitivity—An application of reciprocity," *IEEE Trans. Biomed. Eng.*, vol. BME-16, pp. 15–22, Jan. 1969.

Computationally Effective Algorithm for Robust Weighted Averaging

Jacek M. Łęski* and Adam Gacek

***Abstract*—One of the greatest disadvantages of the weighted signal averaging method is its sensitivity to the presence of noise and outliers in data and the need to estimate the noise variance in all signal cycles. The robust weighted averaging method based on the ε-insensitive loss function is free of these disadvantages, but has a very high computational burden and requires a choice of the insensitivity parameter ε. In this study, a new computationally effective algorithm for robust weighted averaging with automatic adjustment of the insensitivity parameter is introduced.**

***Index Terms*—Fetal ECG, noise reduction, robust weighted averaging, ε-insensitive loss function.**

I. INTRODUCTION

Often the spectra of both biomedical signals and noise overlap for a wide range of frequency. In this case, traditional filtering techniques cause unacceptable signal distortion. However, certain biological systems produce repetitive patterns and, therefore, an averaging in the time domain may be used for noise attenuation. Most types of noise are not stationary, i.e., the noise power measured by the noise variance features some variability. In this case, it is better to use a weighted averaging technique. There are a number of approaches to weighted averaging in literature, including methods based on the minimum energy principle [1], [2], maximizing the signal-to-noise ratio (SNR) using Rayleigh quotient and generalized eigenvalue problem [3], estimating weights adaptatively [4], based on Kalman filter theory [5], [6], with highly quantized weights [7], and robust weighted averaging [8].

One of the greatest disadvantages of traditional and weighted averaging methods is their sensitivity to the presence of outliers caused by, e.g., spike artifacts, including cycles with nondominant morphology, bursts of noisem and baseline shifts. This disadvantage does not occur in robust weighted averaging. Tests performed in [8] showes a very small sensitivity of this method to outliers. However, this approach has serious disadvantages: a very high computational burden and no rule to adjust the insensitivity parameter.

The goal of this paper is to introduce a new robust weighted averaging algorithm with a reduced computational burden and an automatic adjustment of the insensitivity parameter. The solution to the above-mentioned problems will open the possibility of application of the robust weighted averaging in digital processing systems in which rapid processing of results must be used. The examples of these systems are monitoring, exercise, and Holter electrocardiogram (ECG) systems.

II. ROBUST WEIGHTED AVERAGING WITH ITERATIVE LINEAR PROGRAMMING

Let us assume that each signal cycle $x_i(k)$ is the sum of a deterministic (useful) signal $s(k)$, which is the same in all cycles, and a random noise $n_i(k)$ with zero mean and variance for the ith cycle equal to σ_i^2. Thus, $x_i(k) = s(k) + n_i(k)$, where i is the cycle number, $i = 1, 2, \ldots, N$, and k is the discrete time index, $k = 1, 2, \ldots, p$. The weighted average is given by $\sum_{i=1}^{N} w_i x_i(k)$. Let us introduce some vector notations: $\mathbf{x}_i = [x_{i1}, x_{i2}, \ldots, x_{ip}]^\top$ is the ith signal cycle, $\mathbf{v} = [v_1, v_2, \ldots, v_p]^\top$ is the averaged signal, $\mathbf{w} = [w_1, w_2, \ldots, w_N]^\top$ is the weight vector with the properties $\|\mathbf{w}\|_1 = 1, w_i \geq 0$ that leads to an unbiased estimate of the deterministic component. Robust weighted averaging is based on the minimization of the following scalar criterion function [8]:

$$I_{m\varepsilon}(\mathbf{w}, \mathbf{v}) = \sum_{i=1}^{N} (w_i)^m \rceil \mathbf{x}_i - \mathbf{v} \lceil_\varepsilon \tag{1}$$

where

$$\rceil \mathbf{x}_i - \mathbf{v} \lceil_\varepsilon = \sum_{j=1}^{p} \rceil x_{ij} - v_j \lceil_\varepsilon \tag{2}$$

$$\rceil x_{ij} - v_j \lceil_\varepsilon = \begin{cases} 0, & |x_{ij} - v_j| \leq \varepsilon \\ |x_{ij} - v_j| - \varepsilon, & |x_{ij} - v_j| > \varepsilon \end{cases} \tag{3}$$

and $m \in (1, \infty)$ is a weighting exponent parameter.

Using the Lagrange multipliers technique, it is easy to obtain the necessary condition for minimization of (1) with respect to the weights vector [8]

$$\forall_{1 \leq i \leq N} \quad w_i = \left[\rceil \mathbf{x}_i - \mathbf{v} \lceil_\varepsilon\right]^{\frac{1}{1-m}} \Bigg/ \left[\sum_{j=1}^{N} \left[\rceil \mathbf{x}_j - \mathbf{v} \lceil_\varepsilon\right]^{\frac{1}{1-m}}\right]. \tag{4}$$

If we introduce slack variables $\xi_{ij}^+, \xi_{ij}^- \geq 0$, then the averaged signal $\mathbf{v}$ can be obtained by minimization of the following Lagrangian function [8]:

$$\begin{aligned} G_j(v_j) = & \sum_{i=1}^{N} (w_i)^m (\xi_{ij}^+ + \xi_{ij}^-) - \sum_{i=1}^{N} (\mu_{ij}^+ \xi_{ij}^+ + \mu_{ij}^- \xi_{ij}^-) \\ & - \sum_{i=1}^{N} \lambda_{ij}^+ (\varepsilon + \xi_{ij}^+ - v_j + x_{ij}) \\ & - \sum_{i=1}^{N} \lambda_{ij}^- (\varepsilon + \xi_{ij}^- + v_j - x_{ij}) \end{aligned} \tag{5}$$

where $\lambda_{ij}^+, \lambda_{ij}^-, \mu_{ij}^+, \mu_{ij}^- \geq 0$ are the Lagrange multipliers.

Manuscript received January 21, 2003; revised October 6, 2003. *Asterisk indicates corresponding author.*

*J. M. Łęski is with the Division of Biomedical Electronics, Institute of Electronics, Silesian University of Technology, 44-101 Gliwice, Poland, and also with the Institute of Medical Technology and Equipment, 41-800 Zabrze, Poland (e-mail: jl@boss.iele.polsl.gliwice.pl).

A. Gacek is with the Institute of Medical Technology and Equipment, 41-800 Zabrze, Poland (e-mail: adamg@itam.zabrze.pl).

Digital Object Identifier 10.1109/TBME.2004.827953